$N = 16$ Magicity Revealed at the Proton Drip Line through the Study of ^{35}Ca

L. Lalanne,[1,2,*] O. Sorlin,[2,†] A. Poves,[3] M. Assié,[1] F. Hammache,[1] S. Koyama,[4,2] D. Suzuki,[5] F. Flavigny,[6] V. Girard-Alcindor,[2] A. Lemasson,[2] A. Matta,[6] T. Roger,[2] D. Beaumel,[1] Y Blumenfeld,[1] B. A. Brown,[7] F. De Oliveira Santos,[2] F. Delaunay,[6] N. de Séréville,[1] S. Franchoo,[1] J. Gibelin,[6] J. Guillot,[1] O. Kamalou,[2] N. Kitamura,[8] V. Lapoux,[9] B. Mauss,[5,2] P. Morfouace,[2] J. Pancin,[2] T. Y. Saito,[4] C. Stodel,[2] and J-C. Thomas[2]

[1]*Université Paris-Saclay, CNRS/IN2P3, IJCLab, 91405 Orsay, France*

[2]*Grand Accélérateur National d'Ions Lourds (GANIL), CEA/DRF-CNRS/IN2P3, Boulevard Henri Becquerel, 14076 Caen, France*

[3]*Departamento de Física Teórica and IFT-UAM/CSIC, Universidad Autónoma de Madrid, E-2804 Madrid, Spain*

[4]*Department of Physics, The Unviversity of Tokyo, Hongo, Bunkyo-ku, Tokyo 113-0033, Japan*

[5]*RIKEN Nishina Center, 2-1, Hirosawa, Wako, Saitama 351-0198, Japan*

[6]*Normandie Université, ENSICAEN, UNICAEN, CNRS/IN2P3, LPC Caen, 14000 Caen, France*

[7]*Department of Physics and Astronomy, National Superconducting Cyclotron Laboratory, Michigan State University, East Lansing, Michigan 48824, USA*

[8]*Center for Nuclear Study, The University of Tokyo, Hongo, Bunkyo-ku, Tokyo 113-0033, Japan*

[9]*CEA, Centre de Saclay, IRFU, Service de Physique Nucléaire, 91191 Gif-sur-Yvette, France*

(Received 28 February 2023; revised 15 June 2023; accepted 21 July 2023; published 29 August 2023)

The last proton bound calcium isotope ^{35}Ca has been studied for the first time, using the ^{37}Ca$(p,t)^{35}$Ca two neutron transfer reaction. The radioactive ^{37}Ca nuclei, produced by the LISE spectrometer at GANIL, interacted with the protons of the liquid hydrogen target CRYPTA, to produce tritons t that were detected in the MUST2 detector array, in coincidence with the heavy residues Ca or Ar. The atomic mass of ^{35}Ca and the energy of its first $3/2^+$ state are reported. A large $N = 16$ gap of 4.61(11) MeV is deduced from the mass measurement, which together with other measured properties, makes ^{36}Ca a doubly magic nucleus. The $N = 16$ shell gaps in ^{36}Ca and ^{24}O are of similar amplitude, at both edges of the valley of stability. This feature is discussed in terms of nuclear forces involved, within state-of-the-art shell model calculations. Even though the global agreement with data is quite convincing, the calculations underestimate the size of the $N = 16$ gap in ^{36}Ca by 840 keV.

DOI: 10.1103/PhysRevLett.131.092501

Introduction.—Magic nuclei, corresponding to nuclei having special numbers of neutrons and/or protons for which shell gaps are large, feature an enhanced stability as compared to others. Some of the "classical" magic numbers, well identified in stable nuclei (2, 8, 20, 28, 50, 82, and 126), are found to collapse in exotic regions of the chart of nuclides under the combined actions of nuclear forces and correlations (see, e.g., [1–4]). In fact, in the last decades, many experimental and theoretical efforts have proven the disappearance of magic numbers in neutron rich nuclei such as $N = 8$ [5–11], $N = 20$ [12–19], or $N = 28$ [20–25] and also the appearance of new shell closures such as $N = 16$ [26–29], $N = 32$ [30–32], or $N = 34$ [33–35].

Such appearance or vanishing of magic nuclei has generally large impacts in many different fields such as experimental and theoretical nuclear structure, but also astrophysics, fundamental interactions, and symmetries. Each of the known magic numbers is enlightening specific properties of the nuclear force. This is especially remarkable for the magic numbers 28, 50, 82, and 126, which are created by a strong spin-orbit force, or for the so-called harmonic oscillator magic numbers 8, 20 which arise from the short range of the nuclear interaction, in a mass range where the spin-orbit force is not yet dominant. Any other category of magic number likely reveals and constrain the role of nuclear forces or/and symmetry, thus far not or poorly considered. This global understanding of the role of nuclear forces is in turn essential to predict shell structure in unknown regions of the chart of nuclides.

Considering the recently discovered $N = 32$ and 34 neutron (sub)shell closures [30–35] together with the well established ones at $N = 20$ and $N = 28$, the Ca isotopes exhibit thus far the largest number of identified magic nuclei within a single isotopic chain. On the neutron-deficient side of the Ca chain, the high excitation energy of the first 2^+ and 1^+ states in ^{36}Ca, as well as their large neutron-removal spectroscopic factors [36], point to a significant subshell closure at $N = 16$, the size of which remains to be determined.

The magic number $N = 16$ has been identified only around ^{24}O until now, in replacement of $N = 20$ [37], which vanishes around ^{28}O [38,39]. This $N = 16$ magicity was inferred from the combined information of the drop in interaction cross sections [26], the high excitation energy

of the first 2^+ state in ^{24}O [28], and its small quadrupole deformation [29].

In this Letter, we report on the first measurement of the atomic mass and first excited state of the last proton bound Ca isotope ^{35}Ca, produced in the $^{37}\mathrm{Ca}(p,t)^{35}\mathrm{Ca}$ reaction, showing evidence of the magicity of $N = 16$ close to the proton drip line.

Experimental techniques.—The ^{37}Ca nuclei were produced at about 50 MeV/nucleon by fragmentation reactions of a 95 MeV/nucleon $^{40}\mathrm{Ca}^{20+}$ beam, with an average intensity of about 2 $e\mu$A, in a 2-mm thick ^{9}Be target. They were selected by the LISE3/GANIL spectrometer [40], leading to a purity of 20% and mean rate of 3×10^3 pps. They were identified by means of their time-of-flight measurement between one of the two low-pressure multiwire proportional chambers, CATS [41], and the cyclotron radio frequency. The two CATS detectors, placed at a relative distance of 51 cm, were also used to track the ions before their interaction with protons of the liquid hydrogen (LH) cryogenic target CRYPTA [42] of 9.7 mg cm^{-2} at its center, placed at a distance of 67.8 cm downstream of the second CATS detector.

After their interaction with the protons of the LH target, the outgoing ions were detected by a zero degree detection (ZDD) system, composed of an ionization chamber (IC), used for their Z identification, a set of two XY drift chambers, to determine their outgoing angles, and a thick plastic scintillator, mostly used for time-of-flight measurements. The energy and angle of the outgoing triton from the transfer reactions were determined by a set of six MUST2 telescopes [43], covering angles between 3° and 37°. Each of them is composed of a 300-μm thick 10×10 cm double-sided silicon strip detector (DSSSD) with 128 strips on each side backed by sixteen 4-cm thick CsI crystals. The triton identification was performed using their combined energy loss ΔE, measured in the DSSSD and residual energy E, measured in the CsI crystals.

The DSSSDs were calibrated strip by strip, using a triple-alpha source placed at the target position, covering an energy range from 5 to 6 MeV. The CsI detectors were calibrated using the kinematics of the tritons originating from (p,t) reactions with incoming ^{38}Ca and ^{36}Ar nuclei, transmitted in another spectrometer setting (see Fig. 2.3 of [49] in which ^{37}K is also produced), and for which Q values are accurately known from precise mass measurements of the nuclei involved: ^{38}Ca [44], ^{36}Ca [45], ^{36}Ar [46], and ^{34}Ar [47]. With this calibration, atomic masses and uncertainties can be determined from the weighted mean and standard deviation of four independent Q-value measurements performed in the four MUST2 telescopes, located at the closest distance from the target. A similar procedure was applied successfully in Refs. [48,49] to determine the atomic mass of ^{36}Ca using the $^{37}\mathrm{Ca}(p,d)^{36}\mathrm{Ca}$ reaction. Moreover, a further confirmation of the method and of the calibration is obtained from the good agreement between the mass excess of ^{35}K, $\Delta M = -11205(110)$ keV, deduced in the present work from the $^{37}\mathrm{K}(p,t)^{35}\mathrm{K}$ reaction and the known mass of ^{37}K [50] and the precise measurement of $\Delta M = -11172.9(5)$ [50] in a penning trap.

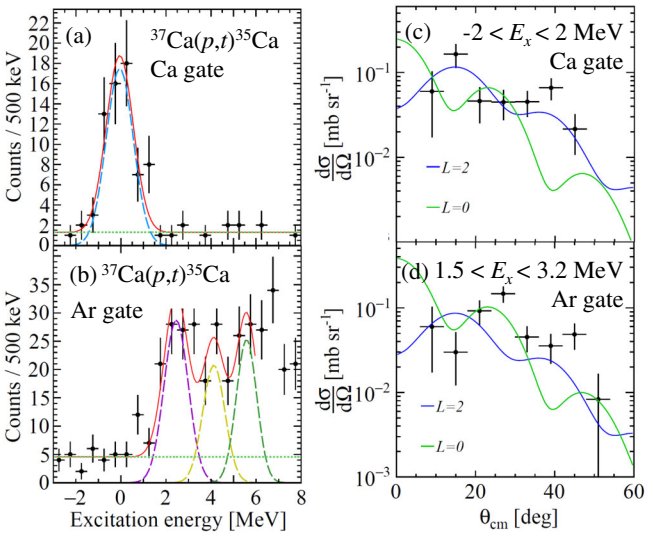

FIG. 1. (a),(b) Excitation energy spectrum of ^{35}Ca obtained from the $^{37}\mathrm{Ca}(p,t)$ transfer reaction with a gate on outgoing Ca (a) and Ar (b). The red lines show the best fit obtained while individual contributions are shown with different color. (c),(d) The experimental differential cross section obtained for the ground state (c) and the first excited state (d) identified in ^{35}Ca using the $^{37}\mathrm{Ca}(p,t)^{35}\mathrm{Ca}$ reaction is shown with the black points. A fit to the cross section is shown using the DWBA calculations performed for an $L = 0$ (green) and an $L = 2$ (blue) transfer.

Results.—The excitation energy E_x of ^{35}Ca, produced by the $^{37}\mathrm{Ca}(p,t)^{35}\mathrm{Ca}$ reaction, was deduced using the missing-mass method from the measurement of the energy and angle of the recoiling triton, detected in MUST2, and an incoming ^{37}Ca identified and tracked in CATS. The ^{35}Ca nucleus can be produced in a bound or unbound state. As the decay product ^{34}K after one proton emission is unbound, the full excitation energy spectrum of ^{35}Ca can be obtained when gating on Ca Fig. 1(a) or Ar Fig. 1(b) isotopes, identified through the measurement of their energy losses in the IC of the ZDD. The red lines in Fig. 1 show the best fit obtained using multiple Gaussian functions plus a background contribution (green dashed line), generated by interactions of the beam particles with the windows of the LH_2 target and determined in a dedicated run with an empty target. The width of each peak used in the fit is constrained by simulations performed with the NPTOOL package [51], the reliability of which is checked from the observed widths of isolated peaks in the reference reactions. The simulated width also matches the ground state value of 700 keV (sigma) in ^{35}Ca, which is found to be the only bound state of ^{35}Ca, as shown in Fig. 1(a).

The Q value of the ^{37}Ca$(p,t)^{35}$Ca reaction has been determined from the energy of the ground state peak and the precise mass value of ^{37}Ca [44]. This leads to a mass excess of $\Delta M(^{35}\mathrm{Ca}) = 4777(105)$ keV. Half of the uncertainty emerges from systematic effects such as the propagation of errors on the measured angle and energy of the tritons and on the energy calibration of the CsI detectors. The other half arises from the low statistics, about 15 counts per detector.

The atomic mass of the ground state of ^{35}Ca, which has isospin components $T_z = -5/2$, $T = 5/2$, and spin $J^\pi = 1/2^+$, can also be estimated from the isobaric multiplet mass equation (IMME) in its quadratic form with T_z. A first attempt to derive the mass excess of ^{35}Ca from the IMME, leading to, $\Delta M(^{35}\mathrm{Ca}) = 4453(60)$ keV, was obtained in [52], which deviates significantly from our value. However, by taking accurate atomic masses of all nuclei involved (that were not available in 1985) and the energy of the $T = 5/2$ isobaric analog state in ^{35}K proposed by Ref. [53], we find $\Delta M(^{35}\mathrm{Ca}) = 4624(50)$ keV. This value agrees within one sigma with the present measurement. Conversely, the atomic mass of ^{35}Ca extrapolated in the last atomic mass evaluation compilation, 5190 (200) keV [54], is 2σ away from our result.

The differential cross sections corresponding to the ground state and to the first excited state of ^{35}Ca are shown in Figs. 1(c) and 1(d). They have been obtained from the distribution of center-of-mass angles, after normalization of its amplitude using the number of incident nuclei, the density of protons in the target, as well as the detection efficiencies (intrinsic and geometrical) of the experimental setup. As the shape of the angular distribution is characteristic of the transferred angular momentum L, distorted wave Born approximation (DWBA) calculations were performed with the code FRESCO [55] assuming $L = 0$ or $L = 2$ angular momentum transfer, using the optical parameters given in [56]. Both calculations of Figs. 1(c) and 1(d) consider only one dominant reaction channel, that are, for $L = 0$ (in green), the direct removal of a pair of neutrons from the $2s_{1/2}$ orbital and, for $L = 2$ (in blue), the direct removal of one neutron from the $2s_{1/2}$ and the other from the $1d_{3/2}$ orbital.

In spite of the limited statistics, it is seen that the shape of the ground state angular distribution of Fig. 1(c) is much better fitted when assuming an $L = 2$ transferred momentum ($\chi^2/\mathrm{ndf} = 10.2/7$), rather than an $L = 0$ one ($\chi^2/\mathrm{ndf} = 27.1/7$), where ndf represents number of degrees of freedom. This $L = 2$ transfer from the $3/2^+$ g.s. of ^{37}Ca, corresponds to the removal of one neutron from the $2s_{1/2}$ and the other from the $1d_{3/2}$ orbital, leaving a single neutron in the $2s_{1/2}$ orbital. Therefore, the g.s. of ^{35}Ca has a spin and parity of $1/2^+$, which is in agreement with the established $1/2^+$ g.s. spin value of the mirror nucleus ^{35}P.

Excited states of ^{35}Ca are visible in the excitation energy spectrum of Fig. 1(b), gated on outgoing Ar. There, the number of contributions used in the fit is guided by the statistical tests of the χ^2 and the p value, as well as the number of ($3/2^+$ and $5/2^+$) states populated in the two-proton transfer quasimirror reaction ^{37}Cl(^{11}B, ^{13}N)^{35}P [57]. The clear rising edge at about 2 MeV in Fig. 1(b) indicates the presence of the first excited state, which is found at 2.24(33) MeV. However, due to the high density of states from 3 MeV onward and the present energy resolution, different fit functions lead to very similar χ^2/ndf (see Fig. 4.38 of Ref. [49]). This precludes a conclusion about the number of higher excited states populated and their exact energies. It also significantly contributes to the increase of the uncertainty of the energy of the first excited state determined in this Letter.

In the mirror nucleus ^{35}P, the first excited state $3/2^+$ at 2.3866(5) MeV [58] has been strongly populated in the two-proton transfer reaction ^{37}Cl(^{11}Be, ^{13}N)^{35}P [57], supporting its tentative spin assignment in ^{35}Ca. Given the large uncertainty on the centroid of the $3/2^+$, one cannot bring valuable conclusions on the mirror energy difference (MED) between the two nuclei.

The differential cross section of the 2.2 MeV excited state, shown in Fig. 1(d), was extracted using a condition on the excitation energy $1.5 < E_x < 3.2$ MeV and requiring an Ar isotope in the ZDD. The data are better fitted with an $L = 0$ transferred momentum ($\chi^2/\mathrm{ndf} = 20.4/7$) than with $L = 2$ ($\chi^2/\mathrm{ndf} = 29.2/7$). This favors spin and parity of $3/2^+$, with two holes in the neutron $2s_{1/2}$ orbital and one neutron in the $1d_{3/2}$ one. Given the present energy resolution, one cannot exclude the contamination from a higher excited state, such as a $5/2^+$ state likely arising from the neutron $1d_{5/2}$ removal (as found at around 3.8 MeV in the mirror nucleus), that may account for the local maximum at about 45°.

Discussion.—The one-neutron separation energy of ^{36}Ca, $S_n(^{36}\mathrm{Ca}) = 19.331(110)$ MeV, was determined by using the present mass measurement of ^{35}Ca and the known value of $\Delta M(^{36}\mathrm{Ca}) = -6483.6\ (56)$ keV [45]. The top panel of Fig. 2 shows the experimental S_n values along the calcium isotopic chain, including the new value of ^{36}Ca. A pronounced decrease of S_n is seen, on top of the odd-even oscillations, after having passed a (sub)shell gap, for $N = 16$, 20, and 28, as well as $N = 32$ and 34 [31,34].

The bottom part of Fig. 2 displays differences of one-neutron separation energies, $\Delta S_n(N) = S_n(N) - S_n(N+1)$ for even-even Ca isotopes. At closed shells, where the effect of pairing is significantly reduced, $\Delta S_n(N)$ is directly related to the amplitude of the shell gap. The maximum value of $\Delta S_n(N)$ along the Ca isotopic chain is reached at $N = 20$ (~7.20 MeV) for the self-conjugate ^{40}Ca nucleus. At $N = 16$, a $\Delta S_n(N)$ of 4.61(11) MeV is obtained, the size of which is very similar to the one at $N = 28$ (~4.80 MeV),

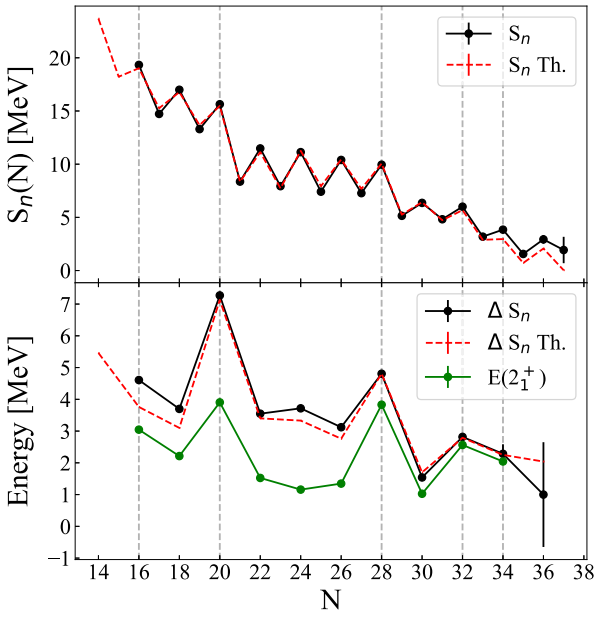

FIG. 2. Top: experimental (black) and theoretical (red) one-neutron separation energy S_n along the calcium isotopic chain. Bottom: ΔS_n and energy of the first 2^+ excited state of even-even Ca isotopes. Theoretical ΔS_n values are shown in red.

significantly larger than that at $N = 32$ (∼2.82 MeV) and twice at large as at $N = 34$ (∼2.28 MeV). This provides a strong evidence of the magicity at $N = 16$, corroborated by the systematics of first 2^+ excited states, also presented in the bottom part of Fig. 2, which follows the same trend as the $\Delta S_n(N)$ values. Note that the spacing between these two curves [$\Delta S_n(N)$ and 2^+] is weaker at $N = 32$ and $N = 34$ than for other magic shells. This is likely due to the fact that the 2^+ states at low energy are more of a pure neutron origin and coincide with the amplitude of the neutron gap, while those at higher energy combine neutron and proton excitations and are more subject to correlations.

Shell-model (SM) calculations have been carried out with the Antoine [59] code using the *sdpf* valence space below $A = 41$ and the *pf* one from $A = 41$ onward. The nuclear, isospin conserving parts, are given by the *sdpf-u-mix* interaction [60] and by the *pfsdg-u* interaction [61], respectively. The two-body matrix elements of the Coulomb interaction are computed with harmonic oscillator wave functions with $\hbar\omega = 41A^{-1/3} - 25A^{-2/3}$. The Coulomb corrections to the single-particle energies are taken from the experimental spectra of the $A = 17$ and $A = 41$ mirror nuclei.

The theoretical $S_n(N)$ and $\Delta S_n(N)$ values are shown in red in Fig. 2. The overall S_n trend is found to be well reproduced by SM calculations. In particular, the theoretical $\Delta S_n(N)$ values are in good agreement with the experimental ones at $N = 20$, 28, 32, and 34. The predicted $\Delta S_n = 3.77$ MeV at $N = 16$, is, however, 840 keV lower than the experimental value of 4.61(11) MeV. $\Delta S_n(N)$ of 3.84 and 4.00 MeV, predicted by the USDA and USDB

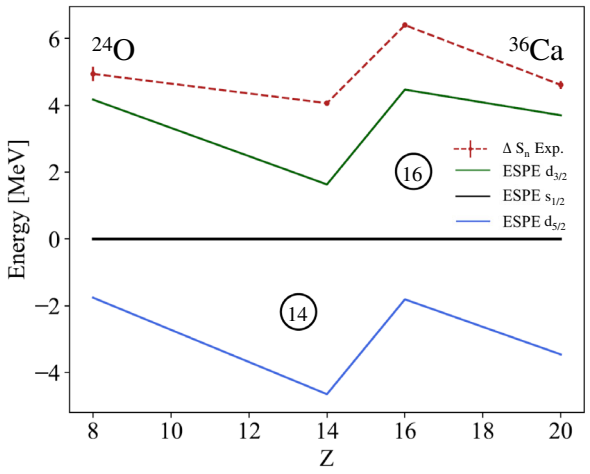

FIG. 3. The effective single particle energies (ESPE) of the neutron $d_{5/2}$, $s_{1/2}$, and $d_{3/2}$ orbitals at $N = 16$ in the *sdpf-u-mix* interaction are shown with the full colored line, relative to the $s_{1/2}$ one. The red dashed lines shows experimental ΔS_n values along $N = 16$ at subshell closures.

interactions [62], are closer but still smaller than the experimental value. In fact this discrepancy can be attributed to a residual defect of the USD family of interactions (notice that USD is the *sd* part of *sdpf-u-mix*) that produce a somewhat (20%) smaller $T = 1$ $(1s_{1/2})^2$ monopole interaction. The ΔS_n value at $N = 16$ measured in this Letter is compatible to the one of ΔS_p at $Z = 16$ in the mirror nucleus ^{36}S of 4.709 MeV. Our SM calculations underestimate the ΔS_p at $Z = 16$ in ^{36}S by the same amount.

The theoretical values of the excitation energy of the $3/2^+$ state in ^{35}Ca, $E_x = 2.38$ MeV obtained with the *sdpf-u-mix* interaction, is in good agreement with the experimental ones of $E_x = 2.24(33)$ MeV, further supporting its spin-parity assignment. The associated MED between ^{35}Ca and ^{35}P is predicted to be of −300 keV, compatible with the shifts of about −250 keV of the 1^+ and 2_1^+ states of the ^{36}Ca-^{36}S mirror pair [36], suggesting a similar origin. Shell model calculation predicts the next shell closure in the Ca isotopes to be at $N = 14$, with a large gap of 5.46 MeV in unbound ^{34}Ca.

The $N = 16$ gap is almost equally large at both edges of the nuclear chart: it amounts to $\Delta S_n = 4.61(11)$ MeV in ^{36}Ca, which lies close to the proton drip line, and to $\Delta S_n = 4.94(20)$ MeV in ^{24}O, which is the last bound oxygen isotope. By applying the $A^{-1/3}$ factor related to the overall compression of the level spacing in atomic nuclei with increasing A, one finds that the $N = 16$ gap is larger in ^{36}Ca than in ^{24}O, viz. $4.61 \times (36/24)^{1/3} = 5.26(12)$ MeV in ^{36}Ca as compared to 4.94(20) in ^{24}O.

Figure 3 shows the evolution of the effective single particle energies (ESPE) of the neutrons $1d_{5/2}$ (blue), $2s_{1/2}$ (black), and $1d_{3/2}$ (green) orbitals at $N = 16$, computed

with the *sdpf-u-mix* interaction, as a function of the proton number. The ESPE of the $1d_{5/2}$ and $1d_{3/2}$ orbitals, given relative to the $2s_{1/2}$ one, directly allows us to determine the predicted amplitudes of the $N = 14$ and $N = 16$ gaps, respectively. Starting from ^{24}O, with the addition of six protons to the $1d_{5/2}$ orbit, the attractive tensor interaction between the two spin-orbit partners reduces the predicted single-particle $N = 16$ gap by about 2.5 MeV at $Z = 14$. The addition of only two more protons to the $2s_{1/2}$ orbit restores the gap at $Z = 16$, while adding four more to the $1d_{3/2}$ proton orbital, brings it back close to the value in ^{24}O.

This predicted evolution of the $N = 16$ gap (green line) is compared in Fig. 3 to experimental ΔS_n values (red dashed line). The ΔS_n values, that corresponds to experimental correlated gaps, are systematically larger than the size of $N = 16$ derived from ESPE. However, the overall trend is similar. It is worth noting that, in spite of a very large gap, ^{32}S does not show significant signs of magicity because of the enhancement of the pairing and quadrupole correlations for this $N = Z$ nucleus.

Conclusion.—The ^{37}Ca$(p, t)^{35}$Ca reaction was performed to obtain the first measurement of the atomic mass of ^{35}Ca, $\Delta M(^{35}\mathrm{Ca}) = 4.777(105)$ keV, as well as the excitation energy of its first excited state at 2.24(33) MeV. The measured differential cross sections together with our shell model calculations support a spin parity of $1/2^+$ for the ground state and $3/2^+$ for the first excited state. The atomic mass was used to infer the amplitude of the gap at $N = 16$ in ^{36}Ca through the determination of $\Delta S_n = 4.61(11)$ MeV, which is very similar to the one of $N = 28$, significantly larger than that at $N = 32$ (~2.82 MeV) and twice at large as at $N = 34$ (~2.28 MeV). This result corroborates the arguments in favor of double magicity of ^{36}Ca from (i) the observation of high-energy 2^+ and 1^+ states and their large C^2S obtained from ^{37}Ca$(p, d)^{36}$Ca [36], (ii) the measured $B(E2, 0_1^+ \to 2_1^+)$ strength in ^{36}Ca [63] that is similar to the ones of the doubly magic ^{40}Ca and ^{48}Ca, and (iii) the small charge radius of ^{36}Ca [64], which is the smallest among all Ca isotopes.

The amplitude of the $N = 16$ gap in ^{36}Ca is also comparable to the one found in ^{24}O, described as a doubly magic nucleus (see, e.g., [28,29]). The fact that $N = 16$ magicity is strongly present at both edges of the nuclear binding gives strong constraints to the proton-neutron interactions involved when adding 12 protons to the *sd* shells. Thus far, the use of state-of-the-art shell-model interactions underestimates the gap derived from ΔS_n by about 0.61 (USDB) to 0.84 MeV (*sdpf-u-mix*). The SM calculation carried out with both interactions predicts the next shell closure of the Ca isotopic chain to be at $N = 14$ in the doubly magic and unbound ^{34}Ca, which is the mirror of the bubble nucleus ^{34}Si [65].

We acknowledge the GANIL facility for provision of heavy-ion ^{40}Ca beam and assistance in using the LISE beamline and its instrumentation. D. S. was supported by the JSPS KAKENHI Grant No. 19H01914. A. P.'s work is supported in part by Grants No. CEX2020-001007-S funded by MCIN/AEI/10.13039/501100011033 and PID2021-127890NB-I00. Support from the NFS Grant No. PHY-2110365 is also acknowledged.

*louis-alexandre.lalanne@cern.ch
†olivier.sorlin@ganil.fr

[1] O. Sorlin and M.-G. Porquet, Prog. Part. Nucl. Phys. **61**, 602673(2008).
[2] A. Gade, Eur. Phys. J. A **51**, 118 (2015).
[3] T. Otsuka, A. Gade, O. Sorlin, T. Suzuki, and Y. Utsuno, Rev. Mod. Phys. **92**, 015002 (2020).
[4] F. Nowacki, A. Obertelli, and A. Poves, Prog. Part. Nucl. Phys. **120**, 103866 (2021).
[5] H. Iwasaki *et al.*, Phys. Lett. B **491**, 8 (2000).
[6] S. Pain *et al.*, Phys. Rev. Lett. **96**, 032502 (2006).
[7] N. Imai *et al.*, Phys. Lett. B **673**, 179 (2009).
[8] A. Krieger *et al.*, Phys. Rev. Lett. **108**, 142501 (2012).
[9] R. Meharchand *et al.*, Phys. Rev. Lett. **108**, 122501 (2012).
[10] C. Morse *et al.*, Phys. Lett. B **780**, 227 (2010).
[11] J. Chen *et al.*, Phys. Rev. C **98**, 014616 (2018).
[12] D. Guillemaud-Mueller, C. Detraz, M. Langevin, F. Naulin, M. de Saint-Simon, C. Thibault, F. Touchard, and M. Epherre, Nucl. Phys. **A426**, 37 (1984).
[13] T. Motobayashi *et al.*, Phys. Lett. B **346**, 9 (1995).
[14] H. Iwasacki *et al.*, Phys. Lett. B **522**, 227 (2001).
[15] Y. Yanagisawa *et al.*, Phys. Lett. B **566**, 84 (2003).
[16] J. R. Terry *et al.*, Phys. Rev. C **77**, 014316 (2008).
[17] H. L. Crawford *et al.*, Phys. Rev. C **93**, 031303(R) (2016).
[18] P. Doornenbal *et al.*, Phys. Rev. C **93**, 044306 (2016).
[19] R. Lica *et al.*, Phys. Rev. C **100**, 034306 (2019).
[20] B. Bastin *et al.*, Phys. Rev. Lett. **99**, 022503 (2007).
[21] C. Force *et al.*, Phys. Rev. Lett. **105**, 102501 (2010).
[22] S. Takeuchi *et al.*, Phys. Rev. Lett. **109**, 182501 (2012).
[23] O. Sorlin, Phys. Scr. T **152**, 014003 (2013).
[24] L. A. Riley *et al.*, Phys. Rev. C **100**, 044312 (2019).
[25] B. Longfellow *et al.*, Phys. Rev. C **103**, 054309 (2021).
[26] A. Ozawa, T. Kobayashi, T. Suzuki, K. Yoshida, and I. Tanihata, Phys. Rev. Lett. **84**, 5493 (2000).
[27] R. Kanungo *et al.*, Phys. Rev. Lett. **102**, 152501 (2009).
[28] C. R. Hoffman *et al.*, Phys. Lett. B **672**, 17 (2009).
[29] K. Tshoo *et al.*, Phys. Rev. Lett. **109**, 022501 (2012).
[30] A Huck, G. Klotz, A. Knipper, C. Miehé, C. Richard-Serre, G. Walter, A. Poves, H. L. Ravn, and G. Marguier, Phys. Rev. C **31**, 2226 (1985).
[31] F. Wienholtz *et al.*, Nature (London) **498**, 346 (2013).
[32] M. Rosenbusch *et al.*, Phys. Rev. Lett. **114**, 202501 (2015).
[33] D. Steppenbeck *et al.*, Nature (London) **502**, 207210 (2013).
[34] S. Michimasa *et al.*, Phys. Rev. Lett. **121**, 022506 (2018).
[35] S. Iimura *et al.*, Phys. Rev. Lett. **130**, 012501 (2023).
[36] L. Lalanne *et al.*, Phys. Rev. Lett. **129**, 122501 (2022).
[37] T. Otsuka, R. Fujimoto, Y. Utsuno, B. Alex Brown, M. Honma, and T. Mizusaki, Phys. Rev. Lett. **87**, 082502 (2001).

[38] A. Revel *et al.*, Phys. Rev. Lett. **124**, 152502 (2020).
[39] S. Bagchi *et al.*, Phys. Rev. Lett. **124**, 222504 (2020).
[40] R. Anne, D. Bazin, A.C. Mueller, J. C. Jacmart, and M. Langevin, Nucl. Instrum. Methods Phys. Res., Sect. A **257**, 215 (1987).
[41] S. Ottini-Hustache *et al.*, Nucl. Instrum. Methods Phys. Res., Sect. A **431**, 476 (1999).
[42] S. Koyama, D. Suzuki, M. Assié, N. Kitamura, L. Lalanne, M. Niikura, H. Otsu, T. Y. Saito, and O. Sorlin, Nucl. Instrum. Methods Phys. Res., Sect. A **1010**, 165477 (2021).
[43] E. Pollacco *et al.*, Eur. Phys. J. A **25**, 287 (2005).
[44] R. Ringle *et al.*, Phys. Rev. C **75**, 055503 (2007).
[45] J. Surbrook *et al.*, Phys. Rev. C **103**, 014323 (2021).
[46] T. Fritioff and G. Douysset, Phys. Scr. **67**, 276 (2003).
[47] F. Herfurth *et al.*, Eur. Phys. J. A **15**, 17 (2002).
[48] L. Lalanne *et al.*, Phys. Rev. C **103**, 055809 (2021).
[49] L. Lalanne, Ph.D. thesis, Université Paris-Saclay, 2021, https://tel.archives-ouvertes.fr/tel-03414417.
[50] C. Yazidjian *et al.*, Phys. Rev. C **76**, 024308 (2007).
[51] A. Matta, P. Morfouace, N. de Séréville, F. Flavigny, M. Labiche, and R. Shearman, J. Phys. G **43**, 045113 (2016).
[52] J. Aysto, D. M. Moltz, X. J. Xu, J. E. Reiff, and J. Cerny, Phys. Rev. Lett. **55**, 1384 (1985).
[53] W. Trinder *et al.*, Phys. Lett. B **459**, 67 (1999).
[54] M. Wang, W. J. Huang, F. G. Kondev, G. Audi, and S. Naimi, Chin. Phys. C **45**, 030003 (2021).
[55] I. J. Thompson, C.R. Phys. **7**, 167 (1988).
[56] Supplemental Material of L. Lalanne *et al.*, Phys. Rev. Lett. **129**, 122501 (2022).
[57] N. A. Orr, W. N. Catford, L. K. Fifiekd, T. R. Ophel, D. C. Weisser, and C. L. Woods, Nucl. Phys. **A477**, 523 (1988).
[58] M. Wiedeking *et al.*, Phys. Rev. C **78**, 037302 (2008).
[59] E. Caurier *et al.*, Rev. Mod. Phys. **77**, 427 (2005).
[60] E. Caurier, F. Nowacki, and A. Poves, Phys. Rev. C **90**, 014302 (2014).
[61] F. Nowacki, A. Poves, E. Caurier, and B. Bounthong, Phys. Rev. Lett. **117**, 272501 (2016).
[62] B. A. Brown and W. A. Richter, Phys. Rev. C **74**, 034315 (2006).
[63] N. Dronchi *et al.*, Phys. Rev. C **107**, 034306 (2023).
[64] A. J. Miller *et al.*, Nat. Phys. **15**, 432 (2019).
[65] A. Mutschler *et al.*, Nat. Phys. **13**, 152 (2017).